

In-Situ Magnetization Reversal Mechanism in Ni Nanowires Investigated by Electron Holography

Arturo Galindo¹ and Arturo Ponce²

¹The University of Texas at San Antonio, San Antonio, Texas, United States, ²Department of Physics and Astronomy. The University of Texas at San Antonio, United States

Increasing interest in ferromagnetic (FM) nanowires (NWs) has inspired considerable research in recent years with the rapid development of information storage technology. The miniaturized dimensions of NWs generate anisotropic magnetic properties due to a competing energy balance between the shape and crystallographic structure. For this reason, the magnetization reversal mechanism in Ni NWs has been greatly investigated as they offer unique advantages in developing high-density magnetic recording media. Consequently, the precise control of the physical properties of FM NWs is a great challenge in nanotechnology. Thus far, the magnetic state of nanomaterials is analyzed using various techniques, however, the magnetic information obtained is limited to the exterior of the nanomaterial. In contrast, a powerful magnetometry technique rests in a specialized transmission electron microscopy (TEM) mode called off-axis electron holography. This technique is equipped to visualize and quantify the local magnetic configuration within and around a magnetic nanomaterial. In effect, we employed off-axis electron holography to perform in-situ magnetization measurements on a single row and individual Ni NWs. This work aims to investigate the magnetization reversal mechanism as a function of an increasing external magnetic field produced by the objective lens. Certainly, capturing the local magnetic state at various magnetic field strengths offers the most detailed look at the magnetization process in Ni NWs.

In electron holography, the interference of a moving electron with the magnetic vector within an FM NW produces a phase shift in the electron wave function following the principles of the Aharonov-Bohm effect [1]. In this way, the total phase recovered provides mutual information on the electrostatic and magnetostatic properties of NWs [2]. As a result, the phase shift can be evaluated provided the respective phases are separated and reconstructed. Moreover, electrochemical depositions of Ni were performed within anodic aluminum oxide (AAO) templates using a commercial Nickel Sulfamate RTU (Technic Inc.) solution at a pH of 4.01. The AAO template was removed in 0.5 M NaOH for 2 h. Subsequently, the NWs were sonicated and collected in a TEM grid. The NWs exhibit a high aspect ratio with a diameter of 80 nm and a length of ~1 μm .

To isolate the magnetostatic contribution, the sample stage was tilted $\pm 16^\circ$. As the maximum tilt angle was reached, a fixed magnetic field was applied. The holograms were acquired after the sample stage was returned to 0° . A digital subtraction process was executed to eliminate the phase shift associated with the electrostatic contribution. The phase reconstruction was carried out using the script HoloWorks 5.0.7 in Digital Micrograph software [3]. A constant amplification of the magnetic phase was preserved to permit comparison at different steps of the magnetization process. Furthermore, the crystal orientation mapping was performed using an automated crystal orientation system that employs a precession electron diffraction unit manufactured by NanoMEGAS.

Initially, an isolated Ni NW displayed a bi-directional spontaneous magnetic flux as seen in Fig. 1(b). The absence of voids and the continuous magnetic flux lines illustrate the dominant shape anisotropy. The flux direction alternates between 0° and 45° forming a wavy behavior. However, once the magnetic flux reaches the NW tip, a sequence of vortex states is generated. This is explained by the varying sizes and orientations of the crystal grains observed in Fig. 1(a). The polycrystalline structure at the tip decreases the magnetocrystalline anisotropy energy, thus the direction of propagation is reversed via a curling mode. Furthermore, the 6 stray field lines observed outside the nanowire suggest that magnetic domain walls are oriented perpendicular to the

long axis of the nanowire [4]. This behavior is also influenced by the remanent field of the objective lens (~ 50 Oe). Correspondingly, a magnetic field of 980 Oe was applied to the sample stage. A unidirectional magnetic flux was observed in Fig. 1(c). The magnetization reversal mechanism in Ni NWs of 80 nm diameter is dominated by the propagation of vortex cores along the longitudinal axis [5]. Hence, various vortex cores were experimentally observed. As the magnetic field increased to 1320 Oe (Fig. 1(d)) the position of the vortex cores moved to the tip of the NW. The amount of 3 and 2 stray field lines observed in Figs. 1(c) & 1(d), respectfully, are thought to emanate from the uncompensated flux closure of the vortex cores. However, the vortex cores disappeared when a magnetic field of 4100 Oe was applied, along with the stray field lines as seen in Fig. 1(e). Finally, magnetic saturation was achieved. The magnetic saturation (M_s) and magnetic induction (B) values were quantified using the recorded phase shift of 7 rad. This corresponds to $M_s = 5.6 \times 10^5$ A/m and $B = 0.65$ T, respectively, which agrees with reported values for Ni NWs [6,7].

In Fig. 2 the hologram of a single row of Ni NWs is observed after tilting the sample stage 21.2° and applying a magnetic field of 16,500 Oe. The magnetic phase is displayed as the colored inset in Fig. 2. In contrast to an isolated NW, the high packing factor promotes strong magnetostatic coupling and dipolar interactions. The magnetic flux propagates at 132° and journeys into adjacent NWs. This analysis demonstrates the complexity of magnetic interactions introduced by the spatial distribution of Ni NWs in AAO templates.

In conclusion, the power of electron holography is demonstrated as a TEM technique that utilizes the concealed physical information encoded within the phase shift of the electron wave to elucidate the magnetic properties of nanomaterials.

The research reported in this publication was supported by the U.S. Department of Defense (DoD) under grant number [W911NF-18-1-0439].

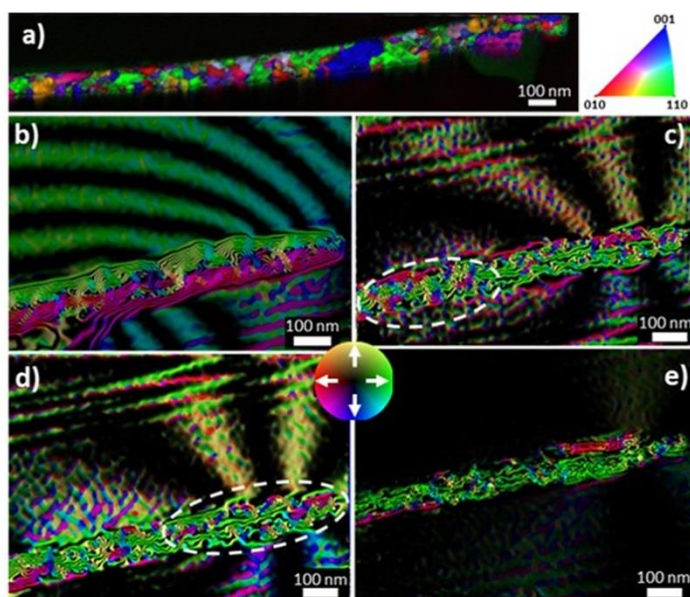


Figure 1. a) Crystal orientation map of a Ni nanowire viewed along the z-axis (parallel to the electron beam path). The color code specifies the presence of (111), (110), and (010) crystal phases for fcc Ni. b) – e) Magnetic phase contour maps of a Ni nanowire exposed to an external magnetic field of 50, 980, 1320, and 4100 Oe, respectively. All magnetic contour maps were amplified by 7X the cosine of the unwrapped magnetic phase. The arrows on the color wheel display the propagation direction of the magnetic flux.

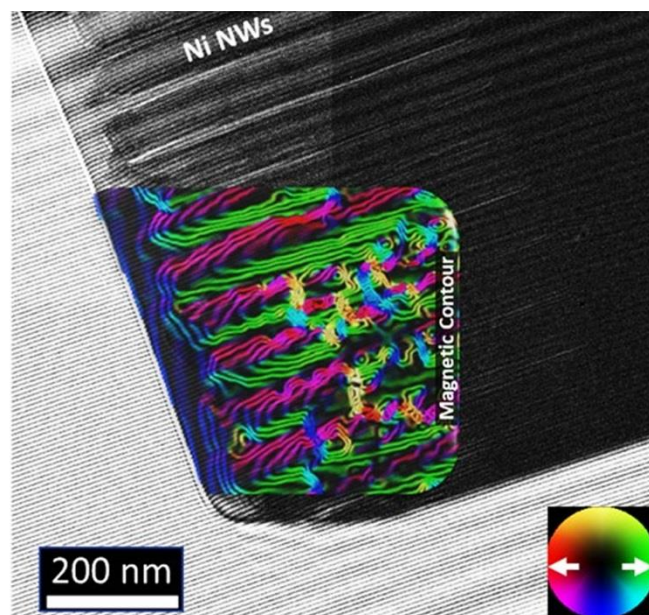


Figure 2. Electron hologram of a single row of Ni nanowires displaying the overlapped interference fringes. The colored inset displays the reconstructed magnetic phase contour amplified at 3X the cosine of the unwrapped magnetic phase. The magnetic flux direction is indicated by the color wheel.

References

- [1] Y. Aharonov and D. Bohm, *Phys. Rev.* **123**, 1511 (1961).
- [2] J. Cantu-Valle, *et.al*, *J. Magn. Mater.* **379**, 294 (2015).
- [3] E. Volkl, *et.al*, *J. Microsc.* **180**, 39, (1995).
- [4] C. Gatel, *et. al*, Dr. Diss. Univ. Paul Sabatier Toulouse III (2020).
- [5] R. Hertel and J. Kirschner, *Phys. B Cons. Matter* **343**, 206 (2004).
- [6] G. L. Drisko, *et. al*, *Nano Lett.* **18**, 1733 (2018).
- [7] E. Ortega, *et.al*, *AIP Adv.* **8**, (2018).